Advances in Water Resources 108 (2017) 397–405

Contents lists available at ScienceDirect

Advances in Water Resources

journal homepage: www.elsevier.com/locate/advwatres

Seasonal dynamics of snail populations in coastal Kenya: Model calibration and snail control

D. Gurarie*, C.H. King, N. Yoon, X. Wang, R. Alsallaq

Department of Mathematics, Applied Mathematics and Statistics and Center for Global Health and Diseases, Case Western Reserve University, 10900 Euclid Avenue, Cleveland, Ohio 44106, USA

ARTICLE INFO

Article history:
Received 11 May 2016
Revised 9 November 2016
Accepted 14 November 2016
Available online 15 November 2016

Keywords:
Model, theoretical
Nonlinear dynamics
Population biology
Schistosomiasis

ABSTRACT

A proper snail population model is important for accurately predicting *Schistosoma* transmission. Field data shows that the overall snail population and that of shedding snails have a strong pattern of seasonal variation. Because human hosts are infected by the cercariae released from shedding snails, the abundance of the snail population sets ultimate limits on human infection. For developing a predictive dynamic model of schistosome infection and control strategies we need realistic snail population dynamics. Here we propose two such models based on underlying environmental factors and snail population biology. The models consist of two-stage (young–adult) populations with resource-dependent reproduction, survival, maturation. The key input in the system is seasonal rainfall which creates snail habitats and resources (small vegetation). The models were tested, calibrated and validated using dataset collected in Msambweni (coastal Kenya). Seasonal rainfall in Msambweni is highly variable with intermittent wet - dry seasons. Typical snail patterns follow precipitation peaks with 2–4-month time-lag. Our models are able to reproduce such seasonal variability over extended period of time (3-year study). We applied them to explore the optimal seasonal timing for implementing snail control.

1. Introduction

Understanding seasonal dynamics of snail populations is important for modeling vector-borne diseases and control interventions where snails serve as the intermediate host, as in schistosomiasis. Indeed, many transmission areas exhibit strong seasonal variations that can affect transmission and control (Kariuki et al., 2004, Sturrock et al., 1990; Remais et al., 2007; Jordan, 1985; Jobin and Michelson, 1967). The classical models of *Schistosoma* transmission (Macdonal, 1965; Barbour, 1978; Anderson and May 1979; Anderson and May 1982; Anderson and May 1985a,b) typically consider only stationary environments and snail populations. That leaves open the question of how seasonality affects the validity of such predictions.

Many ecological and environmental factors drive snail population growth, among them temperature, precipitation, steady or moving water flows, vegetation, and crowding (population density). Earlier works (e.g., Jobin and Michelson, 1967) have described the effect of crowding factors on snail reproduction/growth, while Remais et al. (2007), Guo (1991), Liang et al. (2002), and Woolhouse and Chandiwana (1990a) focus on the role of temperature. The key concept here has been the "temperature-day" (Guo, 1991; Liang et al., 2002; Woolhouse and Chandiwana, 1990a), whereby snails need to accumulate a certain threshold level of days within a suitable temperature "window" to start reproduction. The effect of "temperature-day" accumulation is expressed as a time-lag term in the dynamic snail equation. Different patterns of temperature dependence have been proposed, with an additional contribution by rainfall (Remais et al., 2007; Liang et al., 2002). A recent study (Perez-Saez et al., 2016) further explored multiple environmental drivers (hydrology, climatology et al) that affect snail biology in stationary and seasonal habitats, in particular, the role of population density feedbacks and time lagged environmental inputs.

Our modeling approach takes its cue from those studies, but we focus specifically on snail population dynamics in regions where seasonal precipitation plays the crucial role (Kariuki et al., 2004; Clennon et al., 2004). In such environments (e.g., the southeastern coast of Kenya) rainfall accumulates in water pools (steady of flowing) during the rainy season and creates snail habitats and food resources required for reproduction, a process followed with some delay by an upsurge in the snail population. We assume this time-lag to be due to resource development and the snail maturation processes. In order to reflect this phenomenon, in the present work we have developed two resource-driven snail population models

* Corresponding author: Fax: +1 216 368 5163.
E-mail address: dxg5@case.edu (D. Gurarie).

https://doi.org/10.1016/j.advwatres.2016.11.008
0309-1708/

comprised of young/adult stages, with growth and mortality determined by availability of resource. Two models differ in their setup, the first model (M1) has explicit "resource variable" allocated among stages (via intra-species competition), and resource dependent reproduction / survival. The second model (M2) places emphasis on snail maturation process. Comparison between two systems allows us to assess the relative contribution of two biological factors, "resource dependence" and "maturation time-lag", on snail population dynamics.

We applied our modeling approach to a specific environment and dataset collected in the coastal region of southeastern Kenya (the Msambweni region) (Kariuki et al., 2004; Sturrock et al., 1990; Clennon et al., 2004; Muchiri et al., 1996; Ouma et al., 1989). The local snail species include *Bulinus nasutus* and *Bulinus globosus* - key intermediate hosts for urogenital schistosomiasis. Both species are hermaphroditic, possessing both male and female reproductive organs, and capable of self- or cross-fertilization. A single specimen can invade and populate a new habitat. The eggs are laid at intervals in batches of 5 - 40, each batch being enclosed in a mass of jelly-like material. The young snails hatch after 6 - 8 days and reach maturity in 4 - 7 weeks, depending on the species and environmental conditions. A snail can lay up to 1000 eggs during its life, which may last more than a year. Temperature and food availability are among the most important limiting factors. (see e.g. Woolhouse and Chandiwana, 1990a, Woolhouse and Chandiwana, 1989; Jobin and Michelson, 1967; Webbe, 1968). In our current model, we focus primarily on rainfall as the source of habitat capacity and food resource.

Two models (M1, M2) were calibrated and validated for the Msambweni (rainfall-snail) dataset collected over a 3-year period 1984–1987 (Kariuki et al., 2004; Ouma et al., 1989), using different fitting procedures and data windows.

We applied our models to snail-control analysis, in particular finding the optimal seasonal timing of such control. A molluscicide was implemented numerically as instantaneous removal of a large population fraction, determined by control efficacy. Under favorable conditions (abundant resources) snail populations bounce back to pre-control levels fairly soon, but the overall control effects persist in terms of reduced seasonal snail numbers. We use this "seasonal mean" effect of snail control (population decrease) as a crude proxy for estimating reduced *Schistosoma* transmission from snail to human hosts, and explore optimal seasonal timing of such control.

Overall, our scheme predicts population-level responses to a combination of environmental changes (precipitation) and human intervention (molluscicide). In forthcoming work, we plan to further validate the model, and apply it to *Schistosoma* transmission in coupled human-snail environments.

2. Materials and methods

2.1. Data: Snail environment of the Msambweni region

The field data were collected between March 1984 and July 1986 (Fig. 1). The water bodies were mainly rain-filled ponds and the snail sampling method was by timed collections as described in previous papers (Kariuki et al., 2004; Ouma et al., 1989). Briefly, sampling was conducted by one technician searching each snail site for five minutes using a standard flat wire-mesh scoop with a mesh size of 2 mm. Therefore, only adult snails were enumerated at sampled sites. According to Sturrock et al. (1990), the water levels of ponds fluctuated considerably, leading to large seasonal variation of snail populations. The ponds filled during the rainy season, and snail population peaked with roughly a two-month delay. During the dry season, water levels dropped, with some ponds drying

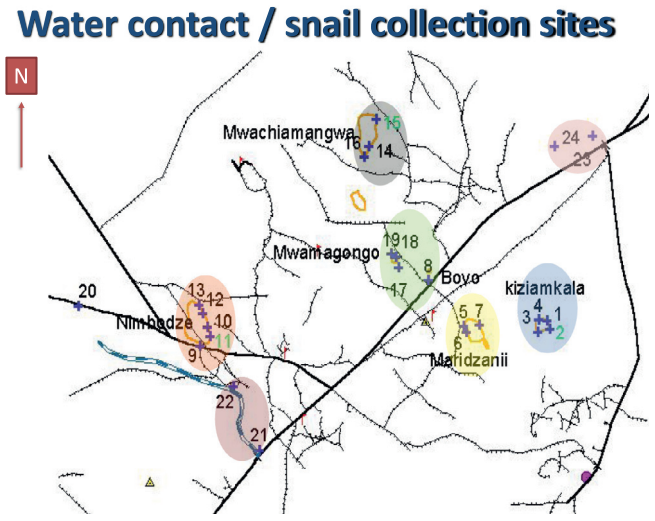

Fig. 1. Msambweni area map with water contact (snail collection) sites marked by crosses numbered 1–24. North is at the top, and the map covers area 5×5 km. The named shaded ellipses mark individual water bodies (seasonal ponds).

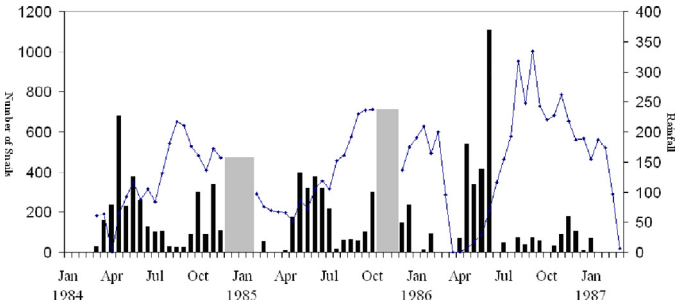

Fig. 2. Rainfall data (solid bar) and snail population (dotted line). Grey bars indicate missing data, snails and rainfall (due to annual staff holidays). For modeling purposes the rainfall data gaps were filled via linear interpolation.

out completely and snail population declining significantly. Fig. 2 shows these patterns over a 3-year period.

Accumulated water level in the ponds creates the vital resource for snail abundance. While other environmental and weather factors (temperature, water turbidity, pH value, aquatic, hydrology of the habitats) can also play significant roles, their effects in the Msambweni area appeared to be more limited. In the follow up study during 2000–2003, Kariuki et al. (2004) found rainfall to be the only reliable predictor of snail populations. In the present study, we use the published Msambweni data for our parameter estimation and model validation.

2.2. Models

Habitat and resources directly impact snail growth rate and survival. Our field studies (Kariuki et al., 2004) have found that long drought significantly reduces snail numbers, but they rebound dramatically after short periods of heavy rain. Typically, after a dry spell, the first rains saturate the soil, then ponds begin to refill. When accumulated rainfall exceeds a certain level, habitat and resources are created that trigger snail population regrowth.

The key dynamic pattern observed in these data is the time lag (two to four months) between the seasonal rainfall peak and snail rebound proliferation (Fig. 2). The rainfall peak typically falls in May, whereas snail abundance (including shedding snails) does not peak until August, September, or even October. Two factors believed to contribute to this delay include delayed resource

development from rainfall, and the time needed for snail maturation from juvenile to adult stage.

The basic principles underlying our model setup are:

(i) Accumulated rainfall creating snail habitat (seasonal pools) and resources (small vegetation consumed by snails) are described by a carrying capacity function $K(t)$. In two models below this function $K(t)$ is responsible for reproduction/growth of resources (M1) or snails (M2).
(ii) A two-stage population structure comprised of young and adult groups that compete for resources. Resource allocation among two groups affects their reproduction and survival.

Such age-structured population dynamics is relevant for several reasons: (i) only adult snails (of sufficient size) can be monitored in the field; (ii) adult snails are responsible for reproduction; (iii) only adult snails contribute to *Schistosoma* transmission (after transitioning to patency).

In the present study, we developed two models of snail population dynamics that focus on different aspects of snail environment and biology. They share common features, including rainfall source for snail habitat and its carrying capacity, and a two-stage (young–adult) snail population dynamic, with group specific mortality, maturation, and reproduction.

These two models, called here the "Resource-limited growth/survival model" and the "Time-lagged development model", emphasize different mechanisms of snail biology. The former makes direct use of environmental resources as dynamic variable, with its allocation resulting in reproduction and survival. The latter model makes implicit use of the available resources via carrying capacity, but it directly models the effect of a developmental time-lag on snail maturation.

3. Resource-limited growth model (M1)

The carrying capacity of snail habitat $K(t)$, is generated via an accumulation-decay process maintained throughout the season. Given a precipitation source $P=P(t)$ and a decay rate θ, we compute $K(t)$ from the differential equation

$$\frac{dK}{dt} = \theta\,(P - K) \tag{1}$$

The decay term accounts for all possible hydrologic losses of habitat and capacity. The additional factor θ in the source, $\theta\,P(t)$ is introduced for technical reasons, (see Appendix A).

The food resource $F(t)$ is assumed to obey a logistic growth equation with carrying capacity $K(t)$and maximal growth rate α

$$\frac{dF}{dt} = \alpha\left(1 - \frac{F(t)}{K(t)}\right)F(t) \tag{2}$$

For large αsolution $F(t)$ would approach $K(t)$, but there would be a time lag between the two functions (see Fig. 3). Two rates, θ, α, of Eqs. (1) and (2) will be estimated along with other biological snail parameters.

Model M1 consists of 3 coupled differential equations for (food) resources, $F(t)$, the young snail population, $Y(t)$, and the adult snail population, $X(t)$. Both reproduction and mortality of each group then depend on the available "resource/snail".

Resource F is assumed to affect snail reproduction and survival; specifically, both will depend on per capita resource level. We further assume F is apportioned between the two age groups in proportion to their consumption rate, population densities (Y – young, X adult), and metabolic needs. We express resource allocation by a single competition parameter, q - the ratio of "adult /young" consumption. The resulting per capita resource variables are

$$f_Y = \frac{F}{Y + qX}(\text{young}); \quad f_X = \frac{qF}{Y + qX}(\text{adult})$$

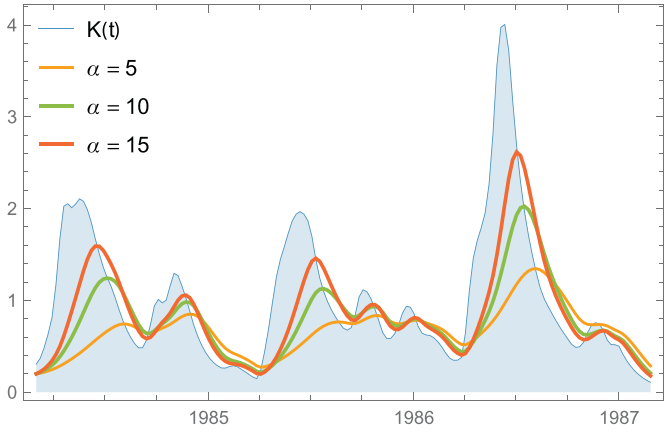

Fig. 3. Accumulated carrying capacity function $K(t)$ of Eq. (1) with $\theta = 7.2$/year (shaded area), and food resource $F(t)$ (thick curves) at 3 values $\alpha = 5$, 10, 20/year. Note that higher α curves $F(t)$ come closer to $K(t)$.

Reproduction rate $\beta(f_X)$ and mortalities $\nu(f_Y)$ (young), $\mu(f_X)$ (adult), are functions of per capita resource. The net result is a coupled differential system for young–adult populations,

$$\begin{cases} \dfrac{dY}{dt} = \beta(f_X)X - (\nu(f_Y) + \tau)Y \\ \dfrac{dX}{dt} = \tau\, Y - \mu(f_X)X \end{cases} \tag{3}$$

with maturation rate τ, period $T = 1/\tau$ (see Appendix A for details). All three rates β, μ, ν are sigmoid (Hill) functions of per capita resource f (= f_X or f_Y),

$$\beta(f) = \frac{\beta_0}{1 + (f_0/f)^{p_B}};$$

$$\mu(f) = \mu_0\left[1 + \left(\frac{f_0}{f}\right)^{p_X}\right]; \quad \nu(f) = \nu_0\left[1 + \left(\frac{f_1}{f}\right)^{p_Y}\right] \tag{4}$$

Each sigmoid function has 3 parameters: (i) "natural" (maximal/minimal) limit value β_0, μ_0, ν_0 (under abundant resource); (ii) half- levelf_0 for adult (β, μ), andf_1 for young (ν); (iii)

Hill exponents p_B; p_X; p_Y (see Fig. 4). Under abundant resource ($f_X \gg f_0$) reproduction would reach its maximal level β_0, while mortalities drop to their "natural" (low) values ν_0, μ_0. Scarce resource ($f_Y \ll f_1$, $f_X \ll f_0$) would decrease reproduction $\beta(f_X)$ and increase mortality for both groups.

The resulting system of Eqs. (1)–(3) has 12 undetermined parameters, which are listed in Table 1. Solution of such system depends on the initial state (F_0, X_0, Y_0) at time $t = 0$. Of those only adult snail X_0 is available from the data. Two other inputs were explored numerically over long term histories. The effect of Y_0 becomes negligible after a relatively short period, so we fixed it at $.5X_0$ in al simulations. Initial resource value F_0 has more persistent effect, so we included it among calibrated model parameters.

Many additional factors can affect snail population dynamics, including competition among multiple snail species, predation, and infection (e.g. *Schistosoma* or other trematodes). Typically, infected snails stop reproduction upon reaching cercaria-shedding patency, which is also associated with higher mortality. However, patent snail numbers for *S. haematobium* species (*Bulinus*) are relatively low, typically below 1–5% of the total adult snail population. So, in the current analysis, we shall ignore the effect of infection on population dynamics.

4. Model of time-lagged population dynamics

In model (M2), we a employ two-stage (young-adult) snail population system, but drop the explicit resource variable $F(t)$.

Table 1
Model parameters, initial range, calibrated values for M1 (mean + SD).

Parameter	Name	Range	ABC Y1-calibration
Loss rate of habitat capacity	θ	3–10/year	8.85 ± 1.17
Relaxation rate of resource	α	3–15/year	8.58 ± .94
Initial resource level	F_0	.05–.5 [a]	.63 ± .139
Maximal snail reproduction rate	β_0	200–2000 /year	230 ± 61
Resource competition factor (adult/young)	q	.1–10 [a]	6 ± 2.98
Natural young mortality	ν_0	5–20/year	19.2 ± 7.41
Natural adult mortality	μ_0	1–10/year	1.56 ± .54
Hill exponent of reproduction	p_B	1–10 [a]	6.21 ± 3.91
Hill exponents of adult mortality	p_X	1–10 [a]	8.51 ± 2.28
Hill exponent of young mortality	p_Y	1–10 [a]	2.1 ± .92
Half- threshold for adult resource	f_0	0–1	.57 ± .056
Half- threshold for young resource	f_1	0–1	.56 ± .15

(1) Gives total egg release/snail / year; the real release could be lower due to shorter reproductive life-span ($1/\mu \approx .5$ year)
[a] Dimensionless parameter

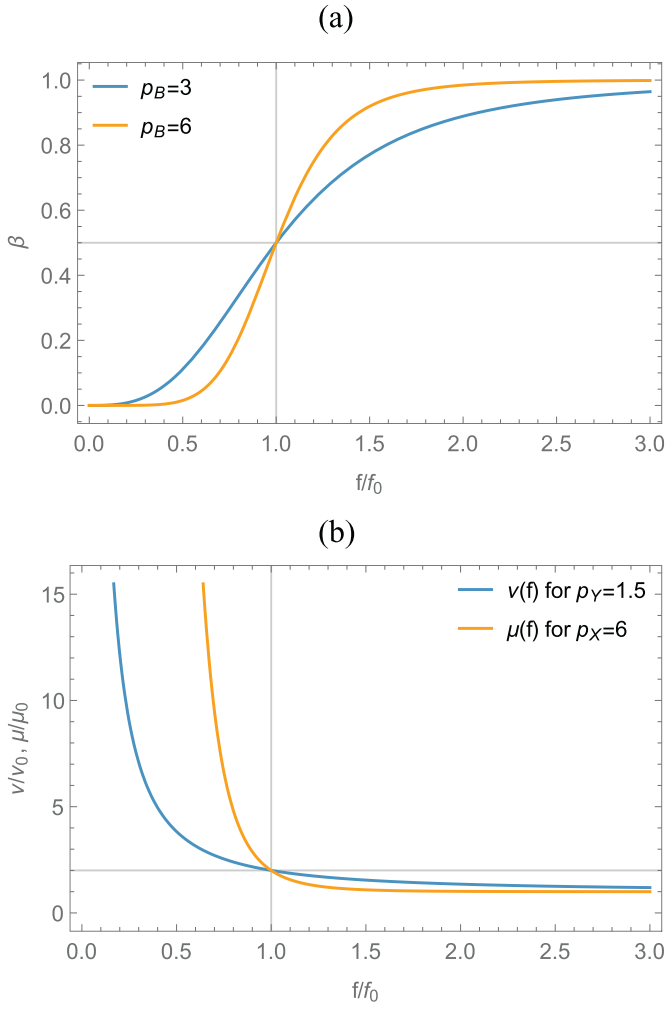

Fig. 4. (a) Resource dependent reproduction function $\beta(f/f_0)$ for different values of the Hill exponent p_B. (b) Young/adult mortality functions: $\nu(f/f_1)$, $\mu(f/f_0)$. Values p_B; p_Y; p_X are taken from the calibrated posterior parameter distribution.

Resource will enter this model implicitly via logistic growth with a maximal reproduction rate β_0, and carrying capacity function $K(t)$, derived from the rainfall via Eq. (1)

$$\beta(X,Y) = \beta_0\left(1 - \frac{Y + qX}{K(t)}\right)X \tag{5}$$

The new $K(t)$ has a different meaning now, instead of "resource capacity", it refers to the "snail population capacity". The mortality rates of the two snail age groups are assumed to be fixed (ν, μ) - (mean mortality), while the snail maturation process is accounted for by time lag factor $T = 1/\tau$. The resulting differential-delay system takes the form

$$\frac{dY}{dt} = \beta(X,Y) - e^{-\nu T}\beta(X,Y)_T - \nu Y$$
$$\frac{dX}{dt} = e^{-\nu T}\beta(X,Y)_T - \mu X \tag{6}$$

Subscript T indicates lagged variables,

$$\beta(X,Y)_T = \beta(X(t-T), Y(t-T)) \tag{7}$$

and factor $e^{-\nu T}$ gives the surviving fraction of a newly-hatched snail egg cluster by the end of the full maturation period.

In both M1 and M2, for calibration and analysis the rainfall and snail data are normalized, so that their mean value over a prescribed period (e.g., year 1) is equal to 1

$$\langle K(t_i)\rangle = 1,\ \langle X(t_i)\rangle = 1.$$

In model M1, the scaling is maintained by the structure of Eqs. (1)–(3), so that

$$1 = \langle P\rangle = \langle K\rangle \approx \langle X\rangle$$

In model M2 however, the carrying capacity function requires an additional scaling factor $K_0 > 1$, so that

$$\beta(X,Y) = \beta_0\left(1 - \frac{Y + qX}{K_0\,K(t)}\right)X \tag{8}$$

The resulting M2 system (6)–(8) with $K(t)$ of Eq. (1) has 7 undetermined parameters listed in Table 2.

3.1. Calibration procedures

Two calibration procedures were adopted: Approximate Bayesian Computation rejection scheme (ABC) and a Markov Chain Monte Carlo (MCMC) approach with Poisson likelihood function (see Appendix E for details). Model M1 was calibrated using both procedures, model M2 was calibrated via the ABC scheme.

In both models, the data (rainfall and snail) were rescaled relative to their mean values over Y1, i.e., mean rainfall $\bar{K} \approx 25$ mm/week, $\bar{K} \approx 360$ (cumulative snail count over all study sites). The rescaled variables, $K(t)/\bar{K}$;$X(t)/\bar{N}$ were used in dynamic simulations and data analysis.

Table 2
Model parameters, initial range, calibrated values for M2 (mean + SD).

Parameter	Name	Range	ABC Y1-calibration	ABC Y1-Y3calibration
Loss rate of carrying capacity function	θ	3–10/year	8.15 ± 1.7	7.7 ± 1.22
Scaling factor for carrying capacity	K_0	1–10	7 ± 1.76	5.7 ± 1.08
Maximal snail reproduction	β_0	100–1000/year	40 ± 9.8	34 ± 7.3
Adult/young competition	q	1–10	1.03 ± .22	1.03 ± .15
Young mortality	ν	5–20/year	14.25 ± 3.34	13.5 ± 2.25
Adult mortality	μ	1–10/year	3.32 ± .83	2 ± .58
Time-lag for maturation	T	2–6 months	1.2 ± .24	1.2 ± .12

5. Approximate Bayesian computation rejection scheme (ABC)

Model M1 has 12 parameters listed in Table 1, whose ranges were taken from data sources or estimated via numeric simulations of the system. We want to select "likely" parameters choices consistent with the snail data (Fig. 2). For each point in the 12-dimensional parameter space $\mathbf{p} = (p_1, \ldots, p_{12})$ we took a particular solution of system (2)-(3)

$$\{F(t|\mathbf{p}), Y(t|\mathbf{p}), X(t|\mathbf{p})\},$$

- function of t and $\mathbf{p}$, evaluated at data points$\{t_k, X_k\}$ (biweekly snail sampling) to get a mean-square error

$$\varepsilon(\vec{p}) = \frac{1}{n}\sum_{1\le k\le n}[X(t_k|\vec{p}) - X_k]^2 \tag{9}$$

Different procedures can be used to select "best-fit" or "likely" parameter choices, ranging from direct minimization of (9) to MCMC.

The ABC calibration scheme employed here proceeded in several steps (see e.g. Sunnåker et al., 2013; Toni et al., 2009). Starting with a uniformly sampled hypercube of Table 1 (uninformed prior), we selects a subset (5%) of best (least-error) parameter choices. This subset was expanded twentyfold by multiplying each one with random factors r_i (in the range $[.8 - 1.2]$), $p_i \to r_i p_i$. The new "posterior cloud" is subjected to similar selection scheme to get the 2nd-step posterior, and the procedure is repeated. After several steps the resulting posterior cloud is expected to settle around likely parameter choices (for details see Appendix C).

The ABC scheme for model M2 (Eqs. (6)–(8)) proceeded in a similar fashion, but this time we used 7 parameters of Table 2.

Different data time windows could be used in model calibration: the entire dataset comprising 3 years of study, or any subset, e.g. Y1, or Y1+Y2. We shall compare the outcomes, and predictive skill for different models and calibration windows.

All numeric codes and procedures for the ABC scheme were implemented on Wolfram Mathematica 10, using its different built-in tools and packages, including differential and differential-delay solvers.

6. Results

6.1. Model calibration

The ABC scheme for models M1 and M2 was run iteratively, and its error distribution (500 best choices) was tracked on each step, along with the error statistics (mean, SD). The error distribution functions tend to approach a stable "limiting pattern", typically after 5–10 steps (see Appendix C for details). The final 500-best choices comprised a posterior cloud (distribution), used for analysis and for dynamic simulations of two models.

Different time-windows were used in the ABC calibration scheme, including Y1-data, combined (Y1-Y2), and the complete 3-year dataset. In the former case (Y1), the remaining history (Y2-Y3) was used for model validation.

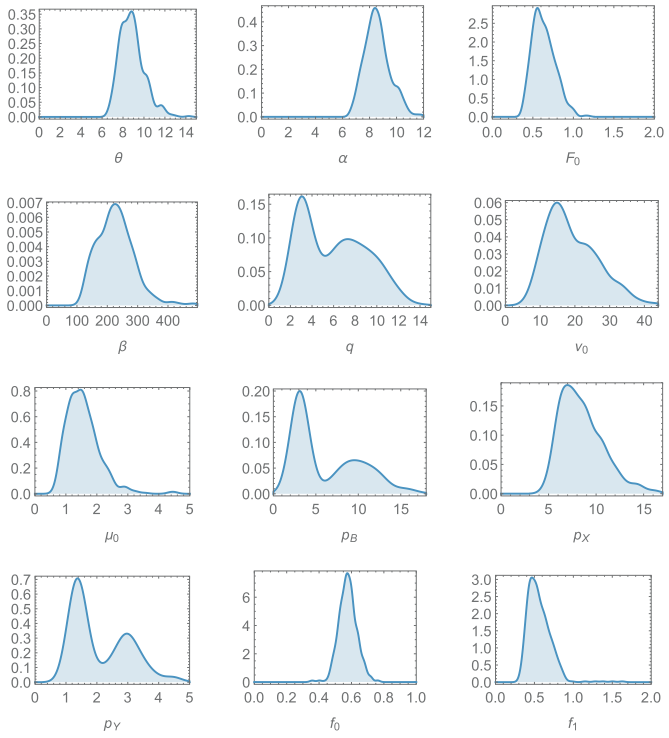

Fig. 5. Marginal parameter distributions of model M1 calibrated via ABC scheme. The scheme employed 500 parameter choices, and the procedure was stabilized after 5 iterative steps.

Fig. 5 shows marginal parameter distributions of M1, estimated vie ABC with Y1-data. They suggest a unimodal (localized) posterior parameter cloud with some (lower level) bimodality for 3 parameters: competition - q, and Hill exponents - p_B (reproduction), p_Y (young mortality). The mean and standard deviation of calibrated parameter are given in Table 1.

The calibrated values are overall consistent with the known biological estimates (see e.g. Clennon et al., 2004; Jordan et al., 1980; Kariuki et al., 2004, Sturrock et al., 2001), e.g., for young and adult snail life-spans ($1/\nu \approx 1$ month, $1/\mu \approx .5$ year), and maximal fecundity (≈ several hundred offspring over an adult life-span).

The same ABC calibration procedure was applied to model M2, using two different time windows: (i) Y1-data alone, (ii) complete 3-year dataset. The calibrated marginal distributions for two schemes are shown in Fig. 6 and Table 2. Once again, most parameters exhibit a localized unimodal pattern.

To test the predictive ability of two models we used Y1-calibration results (posterior distributions), took the 3-year rainfall input and simulated 3-year solution histories for each model by random sampling of their posteriors. The output history envelopes are shown in Fig. 7. Solution envelops of both model captured the essential seasonal snail patterns, but they differed in their predictive skill.

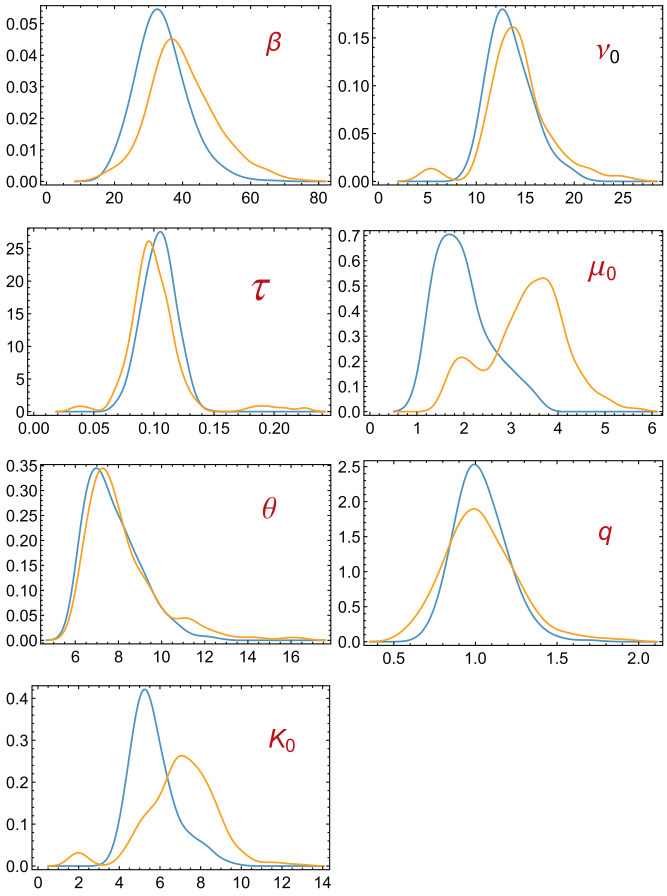

Fig. 6. Marginal parameter distributions of model M2 calibrated (ABC scheme) using Y1-data alone (yellow curves/light color), combined Y1-Y3 dataset (blue curves/dark color). (For interpretation of the references to colour in this figure legend, the reader is referred to the web version of this article.)

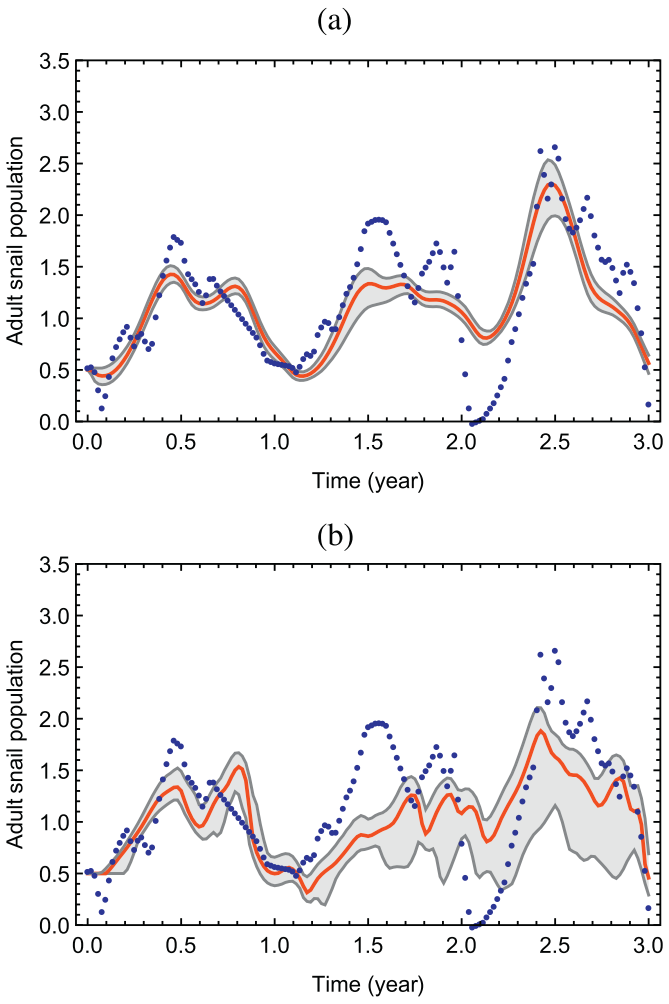

Fig. 7. Solution envelopes of ABC posterior (median and 95% credible interval) for model M1 (panel (a)), and M2 (panel (b)). Data points were rescaled by Y1-mean snail density, $\bar{X} = 360$. The time series (data and model) starts March 1984 and ends February 1987.

Along with ABC-calibration we run an alternative MCMC scheme for model M1, based on Poisson likelihood function, and compared the outcomes of two schemes. They predicted consistent values for some calibrated parameters, but disagreed on other (see Supplementary Appendix E for details). We also tested model M2 for an extended calibration time-window which showed some improvement compared to Fig. 7(b) (see Appendix E).

Models, M1 and M2 share a few common parameters (θ; β; ν_0; μ_0; q), but their meaning is somewhat different in two systems. So not surprisingly, the estimated parameter values differ. The rainfall/habitat decay rate θ is overall consistent for both systems, though function $K(t)$ in M1 refers to carrying capacity of food resource (Eq. (2)), while in M2 it means the carrying capacity of snail population itself. A more striking disparity appears in the estimated reproduction rate β, the M2-parameter β is an order of magnitude lower than M1. The M1-value seems more realistic in terms of egg release by snails, which could count in the hundreds over the snail lifespan. The lower M2-value could possibly be attributed to a different meaning (and count) of "young stage" pool in two systems. Interestingly, the estimated young/ adult mortalities ν_0,μ_0 are fairly consistent in both systems, though in M1 they refer to "natural survival" (under abundant resources), while in M2 they represent the "mean survival rate". Resource competition factor q however, is several times higher for M1 than M2.

Both models capture the essential seasonal variability of resource-dependent snail populations. But they differ in their predictive skill. Indeed, model 1 calibrated via Y1-window data alone is capable of predicting the entire 3-year history with reasonable accuracy (Fig. 7(a)). In fact, the Y1-window calibration for M1 is fairly close to the Y1-Y3 window calibration. Unlike model M1, the M2-prediction horizon doesn't seem to extend far beyond the time-window employed in its calibration (cf., Fig. 7(b) vs. Fig. 7 of Appendix E).

The biggest discrepancy between observed data and the models' predictions appears at the end of Y2, where both models underestimated abrupt changes in the snail population, in terms of its steep rise and fall (Fig. 7). One can attribute this discrepancy to missing (incomplete) rainfall data, which had to be inferred via linear interpolation. In reality these missing parts of the dry season have experienced zero precipitation, resulting in a sharp loss of snail habitat and population. Another possible source of this discrepancy in snail numbers could be due to adult snail disappearance via aestivation in a drying pool environment, discussed below.

6.2. Optimal timing of molluscicide

Snail control (molluscicide) is currently considered a viable option to supplement human chemotherapy for prevention of schistosomiasis. The respective snail-to-human and human-to snail forces of infection (FOI), as well as transmission intensity, depend on snail population density. So any sustained reduction of snail numbers is expected to bring about gradual reduction of human infection

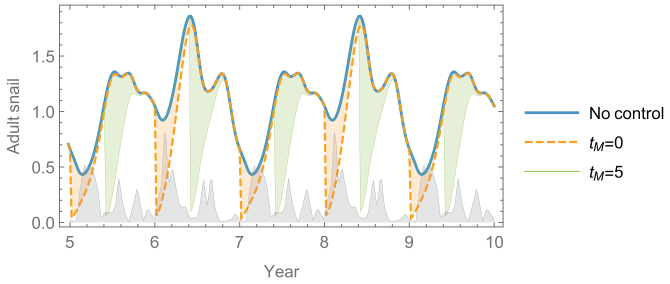

Fig. 8. Long term effect of annual molluscicide simulated by model M1. The rainfall input for simulations was obtained by the 2-year periodic extension of the Kenyan dataset 1984–85 (shaded gray at the bottom). Each history was run over a simulated 10-year period, and the plot shows the last 5 years. The thick blue (dark) curve is snail population's natural history $X(t)$ without control. The yellow (dashed) and green (thin) curves correspond to different molluscicide timing: start of the season (March) $t_M = 0$ (yellow), and midseason (July) $\tau_M = 5$ months (green). Shaded yellow, green areas show snail loss due to molluscicide relative to the unperturbed (natural) curve $X(t)$. (For interpretation of the references to colour in this figure legend, the reader is referred to the web version of this article.)

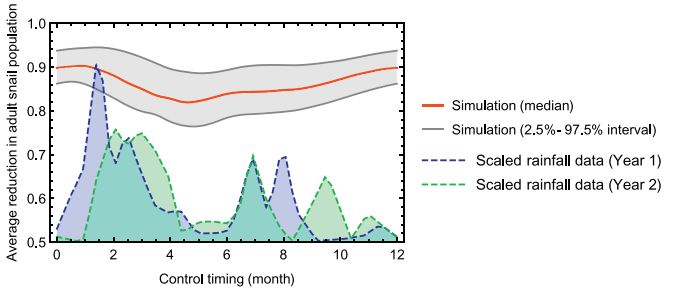

Fig. 9. Relative annual mean snail reduction ρ_C for different control timing: $0 < t_M < 1$ year. Shaded regions indicate rainfall on odd (Y1) and even (Y2) years. Optimal timing for molluscicide occurs between months 4 and 6, past the first rainfall peak; it gave $\approx$ 20% reduction, as opposed to 10% reduction for the start-of-season strategy (i.e., molluscicide preceding peak rainfall). The computed envelope was based on 500 likely parameter choices.

(King et al., 2015). When averaged over a multi-year control period, the relative reduction of snail numbers could serve as a crude proxy of reduction of snail-to-human FOI.

More accurate accounting of the effect of molluscicide would require a coupled human-snail transmission system (see e.g. Gurarie et al., 2016) but we shall postpone it to a future study. Our main goal here is to explore the effect of seasonally adjusted molluscicide on snail abundance.

A dynamic snail model capable of predicting population response to abrupt changes (e.g., molluscicide-mediates clearance) is essential for such analysis. Here we employ the calibrated model M1 over Y1 time window. The key input in our system is seasonal rainfall $P(t)$. Fig. 2 shows highly irregular rainfall pattern, but two seasonal peaks are clearly discernable, with a strong peak in the early rainy season (March-June long rains) and a weaker peak in the later rainy season (October-November short rains) each year.

We are interested in the long term effect of seasonally administered molluscicide, which requires long term rainfall input. There are different ways to generate a multiyear rainfall (Appendix C). Here we employ the Kenyan rainfall Fig. 2 (e.g., Y1 or Y1+Y2), and extend it periodically. That is, we project a biennial extension of rainfall data based on Y1+Y2.

Molluscicide - a release of chemical into the snail environment- will rapidly kill a large number of snails, both young and adults. In our numeric code, we implement this via an instantaneous change of snail variables, $X(t_0) \to \varepsilon X(t_0)$, $Y(t_0) \to \varepsilon Y(t_0)$, at the time t_0 of molluscicide release. Here $0 < \varepsilon < 1$ - the fraction of surviving snails- measures molluscicide efficacy. In the simulations below, we take $\varepsilon = .05$. We expect that following any sharp drop in snail population, given their reproductive potential, snail numbers would rebound to precontrol levels under favorable conditions, but the overall seasonal mean snail number (a crude proxy for transmission potential) would be lowered (due to the molluscicide effect) compared to its natural mean abundance. Molluscicide strategies differ by their seasonal timing the fraction of the year that has passed since March (season start), or $0 < t_M \leq 12$ months.

Fig. 8 illustrates 3 long term histories on the background of periodic (biennial) rainfall pattern (shaded gray) simulated over 10-year period (only last 5 years are shown). One of the curves (blue) is unperturbed "natural" snail population dynamics as predicted by calibrated model for a particular parameter choice; the yellow curve represents a "start of season" molluscicide application, $t_M = 0$ (March), while the green curve is a "midseason" molluscicide application $t_M = 5$ month (July). Shaded regions demonstrate the related abrupt drop and rebound of snail numbers. We then measured the effect of molluscicide by relative value of the reduced (seasonal mean) snail level $X_C(t)$, due to molluscicide, relative to its natural uncontrolled (natural) function $X(t)$,

$$\rho_C = \frac{\langle X_C(t) \rangle}{\langle X(t) \rangle} \tag{10}$$

Given large seasonal variability, the timing of control sessions and their frequency could have a significant impact on ρ_C. The question of optimal seasonal timing can now be explored by long term simulations of molluscicide on the background of a prescribed (periodic, quasi-periodic) rainfall function $P_T(t)$. We used the calibrated model M1 (Eqs. (1)–(3)), and took a sample of its "best-fit" (likely) parameter choices to account for model uncertainties. For each parameter choice, we ran a multi-year molluscicide regimen and varied its annual seasonal timing. Molluscicide was implemented on a fixed seasonal timing t_M, regardless of rainfall variability (shifting peaks) in subsequent years. Such strategy is one possible choice that could be explored with our models. Other possible strategies could be implemented, e.g., linking molluscicide to specific rainfall peaks/troughs of that could vary from one season to another.

The results shown in Fig. 9 identify midseason $4 < t_M < 6$ month (June-July) as an optimal timing for an annual molluscicide regimen. Such t_M could attain up to 20% mean seasonal reduction of ρ_C. In contrast, early season timing ($t_M = 0$) gives only 10% reduction. The time histories in Fig. 8 corroborate this finding, as indicated by the optimal green curve vs. the suboptimal yellow curve. The predicted optimal timing for molluscicide follows the early-season rain peak by a 2–3-month lag, which is roughly the time of the post-rain snail peak for unperturbed (natural) histories (see Figs. 8, and 9).

7. Discussion and conclusions

Multiple factors affect snail population biology in variable habitats, and different modeling approached were proposed to address these issues (Kariuki et al., 2004, Jobin and Michelson, 1967; Webbe, 1968; Jordan et al., 1980; King et al., 2015; Macdonald et al., 1973; Woolhouse and Chandiwana, 1990b). A recent work Perez-Saez et al. (2016) in particularly, attempts to assess multiple geographic, environmental and climatological factors of snail ecology on regional and country scales. In our paper we take a specific local environment - Kwale County in coastal Kenya and its seasonal ponds, but we attempt to explore the essential biological mechanisms underlying snail response to environmental conditions.

The key contributing factor in coastal Kenya comes from the rainfall, which alternates between wet and dry seasons. The data

collected in several Kwale sites show that peak periods of rainfall are followed by rebound of snail numbers with a 2–4 month time lag.

In this study, we developed two models that attempt to reproduce such patterns of snail population dynamics, and applied different calibration schemes these systems. The first model (M1) made explicit use of a food resource variable, which was posited to affect snail reproduction, maturation, and mortality. The second model (M2) dropped the explicit resource variable, but accounted for it implicitly via snail carrying capacity function. The M2 model, however, had a more realistic snail maturation process implemented via differential-delay equations. The key input in both systems was accumulated rainfall, which affected the model performance either via capacity of food resources (M1), or as carrying capacity of the snail population (M2).

The two models differed in the number of parameters twelve for M1 and seven for M2. These partly overlapped and allow some comparison. Models were calibrated by two different calibration schemes (ABC, MCMC), and different calibration runs employed either complete or partial datasets. The goal was to assess the validity and predictive skill of each model and parameter-fitting procedure, and to apply the optimally-fitted models to control analysis (molluscicide). The analysis of calibrated parameters has shown strong correlations among them, so the “effective” number of parameters could be lower (for details, see Appendix C). The ABC scheme developed in the paper offers one possible way to address data and models uncertainties. For alternative approaches, we refer to King et al. (2008), Wu et al. (2013) and Sunnåker et al. (2013).

Both models are capable of reproducing the gross features of seasonal variation, but their accuracy and predictive ability varied. Both predicted a bimodal snail abundance pattern during Y1, following each of the two rainy seasons, although the second peak was slightly delayed. More significant discrepancies arose at the end of Y2, where both models underpredicted the observed steep rise and fall in snail numbers. There are several plausible explanations of such a disconnect. The rainfall data by the end of Y1 and Y2 were missing due to annual staff vacations, and we inferred values for the data gaps via linear interpolation. In reality, the end of each season (Y1, Y2) could have had no rain. As a result, the habitat carrying capacity function (for resources or snails) could have undergone more severe declines than predicted by our interpolated models, yielding a much more pronounced drop in snail numbers (Fig. 7). It is possible that we have missed some important aspects of snail biology and environment that would be responsible for such drop. It is also possible the steep drop in data was due to undercounts of snail numbers due to dry-season aestivation through to the next rain season (see Jobin and Michelson, 1967; Jordan et al., 1980). The gradual transition between Y2 and Y3 predicted by our model simulation could reflect “unobservable” aestivating snail numbers. Indeed, model M1 has accurately predicted snail rebound in Y3 following their steep decline, although it was calibrated with Y1 data only (Fig. 7(a)).

Overall, M1 seems to fit the data better than M2, in terms of long range predictions (beyond its calibration time-window). The key difference between two systems was resource-driven reproduction and mortality (M1) absent in M2. One could draw some conclusions regarding relative impact of “resource-dependence” vs. “developmental time-lag”. Let us note however, all such conclusions are provisional to the current setup, which has its own limitation, “fixed” maturation rate, rather than more realistic system with resourse-dependent reproduction, survival and maturation. A future development may include additional features in M1, M2. A more comprehensive comparison between different approaches and the underlying assumptions (resource dependence, maturation pattern) could involve systematic analysis of the "degrees of complexity" in the reproduction and mortality rates (testing all combinations of fixed vs. resource dependent rates (see e.g. Toni and Stumpf, 2010).

The advantage of M2 model is its relative simplicity, (fewer variables and parameters, a single input - hypothetical carrying capacity function $K(t)$. In such form M2 could potentially be fitted to other environments without direct recourse to precipitation or “resource development”.

Dynamic snail population models are essential for control analysis of such systems, as they allow one to predict population responses under adverse conditions, environmental changes, or human interventions (molluscicide). So far, we have employed our model to examine the effect of seasonally adjusted molluscicide to identify the best timing for annual interventions. Such snail control is currently considered a viable option to supplement human chemotherapy for schistosomiasis. As we have shown, snail density and the infected and patent snail subpopulations contribute directly to the force of human infection - the rate of new worm accumulation in at-risk communities.

One could go further along these lines and explore long term (multi-seasonal) effect of molluscicide for an observed rainfall, so as to reduce snail survival and growth under favorable or adverse environmental conditions. In practice, the ultimate goal of snail control is to bring down the *Schistosoma* transmission. Our next goal is to apply our current seasonal snail population model to *Schistosoma* transmission systems developed in previous papers (Wang et al., 2012; Gurarie et al.; 2010; Gurarie et al., 2015; Gurarie, 2014; Gurarie et al., 2016).

The methodology of resource-driven growth could be extended to other environments and weather patterns. In each case, one needs to identify the essential mechanisms and specific environmental factors that affect snail dynamics. For instance, flowing snail habitats (see e.g. (Jordan, 1985)) will likely need a different modeling design and inputs specific for the area, beyond rainfall. Other improvements in modeling could include a better account of hydrology and environmental resources as they affect the carrying capacity function $K(t)$ (1). There are several ways to improve the biological part of the system, for instance making maturation process resource dependent, along with reproduction/survival (see e.g. Woolhouse and Chandiwana, 1990b; Remais et al., 2007). We plan such development of models and methodologies for the future study.

Acknowledgments

This work was funded by the Schistosomiasis Consortium for Operational Research and Evaluation (SCORE), based at the University of Georgia, USA, and by the Children’s Investment Fund Foundation (UK) (“CIFF”) through a grant to the Neglected Tropical Diseases Modeling Consortium at Warwick University, UK. The views, opinions, assumptions or any other information set out in this study are solely those of the authors and should not be attributed to CIFF or any person connected with CIFF. The funders had no role in study design, data collection and analysis, decision to publish, or preparation of the manuscript.

We also acknowledge valuable inputs from the editors and reviewers which helped us to make marked improvements in the paper’s content and presentation.

Supplementary materials

Supplementary material associated with this article can be found, in the online version, at doi:10.1016/j.advwatres.2016.11.008.

References

Anderson, RM, May, RM, 1979. Prevalence of Schistosome infections within molluscan populations - observed patterns and theoretical predictions. Parasitology 79, 63–94.

Anderson, RM, May, RM, 1982. Population-dynamics of human helminth infections - control by chemotherapy. Nature 297, 557–563.

Anderson, RM, May, RM, 1985. Herd-immunity to helminth infection and implications for parasite control. Nature 315, 493–496.

Anderson, RM, May, RM, 1985. Helminth infections of humans - mathematical-models, population-dynamics, and control. Adv. Parasitol 24, 1–101.

Barbour, AD, 1978. Macdonalds model and transmission of bilharzia. Trans. R. Soc. Trop. Med. Hyg 72, 6–15.

Clennon, JA, King, CH, Muchiri, EM, Kariuki, HC, Ouma, JH, Mungai, P, et al., 2004. Spatial patterns of urinary schistosomiasis infection in a highly endemic area of coastal Kenya. Am. J. Trop. Med. Hyg 70, 443–448.

Guo, Y, 1991. Schistosome biology, prevention and cure of Schistosomiasis. In: Mao, S. (Ed.), Snail Biology. People Health Press, Bejing, pp. 260–273.

Gurarie, D, 2014. CH King population biology of *Schistosoma* mating, aggregation, and transmission breakpoints: more reliable model analysis for the end-game in communities at risk. PLoS One 9, e115875. https://doi.org/10.1371/journal.pone.0115875.

Gurarie, D, King, CH, Wang, X, 2010. A new approach to modelling schistosomiasis transmission based on stratified worm burden. Parasitology 137, 1951–1965. https://doi.org/10.1017/S0031182010000867.

Gurarie, D, King, CH, Yoon, N, Li, E, 2016. Refined stratified-worm-burden models that incorporate specific biological features of human and snail hosts provide better estimates of Schistosoma diagnosis, transmission, and control. Parasites Vectors. BioMed 9, 428. https://doi.org/10.1186/s13071-016-1681-4.

Gurarie, D, Yoon, N, Li, E, Ndeffo-Mbah, M, Durham, D, Phillips, AE, et al., 2015. Modelling control of *Schistosoma haematobium* infection: predictions of the long-term impact of mass drug administration in Africa. Parasit Vectors 8, 529. https://doi.org/10.1186/s13071-015-1144-3.

Jobin, WR, Michelson, EH, 1967. Mathematical simulation of an aquatic snail population. Bull. World Health Org 37, 657–664 D - NLM: PMC2554372 EDAT-1967/01/01 MHDA- 1967/01/01 00:01 CRDT- 1967/01/01 00:00 PST - ppublish.

Jordan, P, Christie, JD, Unrau, GO, 1980. Schistosomiasis transmission with particular reference to possible ecological and biological methods of control. A Rev. Acta. Tropica. 37 95–135.

Jordan, P., 1985. The St Lucia Project. Cambridge University Press, Cambridge.

Kariuki, HC, Clennon, JA, Brady, MS, Kitron, U, Sturrock, RF, Ouma, JH, et al., 2004. Distribution patterns and cercarial shedding of *Bulinus nasutus* and other snails in the Msambweni area, Coast Province, Kenya. Am. J. Trop. Med. Hyg. 70, 449–456.

King, AA, Ionides, EL, Pascual, M, Bouma, MJ, 2008. Inapparent infections and cholera dynamics. Nature 454, 877–880. https://doi.org/10.1038/nature07084.

King, CH, Sutherland, LJ, Bertsch, D, 2015. Systematic review and meta-analysis of the impact of chemical-based mollusciciding for control of Schistosoma mansoni and S. haematobium Transmission. PLoS Negl. Trop. Dis. 9, e0004290. https://doi.org/10.1371/journal.pntd.0004290.

Liang, S, Maszle, D, Spear, RC, 2002. A quantitative framework for a multi-group model of Schistosomiasis japonicum transmission dynamics and control in Sichuan. China. Acta Tropica. 82, 263–277.

Macdonal, G, 1965. Dynamics of helminth infections with special reference to schistosomes. Trans. R. Soc. Trop. Med. Hyg 59, 489–506.

Macdonald, F, Clarke Vde, V, Gaddie, P, Atkinson, G, 1973. Report on a large-scale attempt at control of bilharziasis by combined mass treatment and intensive snail control. Cent. Afr. J. Med 19, 22–32.

Muchiri, EM, Ouma, JH, King, CH, 1996. Dynamics and control of *Schistosoma haematobium* transmission in Kenya: an overview of the Msambweni Project. Am. J. Trop. Med. Hyg 55, 127–134.

Ouma, JH, Sturrock, RF, Klumpp, RK, Kariuki, HC, 1989. A comparative-evaluation of snail sampling and cercariometry to detect Schistosoma-Mansoni transmission in a large-scale, longitudinal field-study in Machakos, Kenya. Parasitology. 99, 349–355.

Perez-Saez, J, Mande, T, Ceperley, N, Bertuzzo, E, Mari, L, Gatto, M, et al., 2016. Hydrology and density feedbacks control the ecology of intermediate hosts of schistosomiasis across habitats in seasonal climates. Proc. Natl. Acad. Sci 113, 6427–6432.

Remais, J, Hubbard, A, Wu, ZS, Spear, RC, 2007. Weather-driven dynamics of an intermediate host: mechanistic and statistical population modelling of Oncomelania hupensis. J. Appl. Ecol 44, 781–791. https://doi.org/10.1111/j.1365-2664.2007.01305.x.

Sturrock, RF, Diaw, OT, Talla, I, Niang, M, Piau, JP, Capron, A, 2001. Seasonality in the transmission of schistosomiasis and in populations of its snail intermediate hosts in and around a sugar irrigation scheme at Richard Toll, Senegal. Parasitology 123, S77–S89 Suppl.

Sturrock, RF, Kinyanjui, H, Thiongo, FW, Tosha, S, Ouma, JH, King, CH, et al., 1990. Chemotherapy-based control of schistosomiasis haematobia. 3. Snail studies monitoring the effect of chemotherapy on transmission in the Msambweni area, Kenya. Trans. R. Soc. Trop. Med. Hyg. 84, 257–261.

Sunnåker, M, Busetto, AG, Numminen, E, Corander, J, Foll, M, Dessimoz, C, 2013. Approximate bayesian computation. PLoS Comput. Biol 9, e1002803.

Toni, T, Stumpf, MP, 2010. Simulation-based model selection for dynamical systems in systems and population biology. Bioinformatics 26, 104–110.

Toni, T, Welch, D, Strelkowa, N, Ipsen, A, Stumpf, MP, 2009. Approximate Bayesian computation scheme for parameter inference and model selection in dynamical systems. J. R. Soc. Interface 6, 187–202.

Wang, X, Gurarie, D, Mungai, PL, Muchiri, EM, Kitron, U, King, CH, 2012. Projecting the long-term impact of school- or community-based mass-treatment interventions for control of *Schistosoma* infection. PLoS Negl. Trop. Dis 6, e1903. https://doi.org/10.1371/journal.pntd.0001903.

Webbe, G., 1968. Quantitative studies of intermediate host populations in the transmission of schistosomes. In: Proceedings of the Royal Society of Medicine, 61, p. 455.

Woolhouse, M, Chandiwana, S, 1990b. Temporal patterns in the epidemiology of schistosome infections of snails: a model for field data. Parasitology 100, 247–253.

Woolhouse, ME, Chandiwana, SK, 1989. Spatial and temporal heterogeneity in the population dynamics of *Bulinus globosus* and *Biomphalaria pfeifferi* and in the epidemiology of their infection with schistosomes. Parasitology 98, 21–34.

Woolhouse, MEJ, Chandiwana, SK, 1990a. Population-dynamics model for Bulinus–Globosus, intermediate host for Schistosoma-Haematobium, in river habitats. Acta Tropica 47, 151–160.

Wu, J, Dhingra, R, Gambhir, M, Remais, JV, 2013. Sensitivity analysis of infectious disease models: methods, advances and their application. J. R. Soc. Interface 10 20121018.